



Simplification of Visual Rendering in Simulated Prosthetic Vision Facilitates Navigation

Victor Vergnieux, Marc J.-M. Macé, and Christophe Jouffrais

Université de Toulouse and CNRS, IRIT, UMR5505, Toulouse, France

Abstract: Visual neuroprostheses are still limited and simulated prosthetic vision (SPV) is used to evaluate potential and forthcoming functionality of these implants. SPV has been used to evaluate the minimum requirement on visual neuroprosthetic characteristics to restore various functions such as reading, objects and face recognition, object grasping, etc. Some of these studies focused on obstacle avoidance but only a few investigated orientation or navigation abilities with prosthetic vision. The resolution of current arrays of electrodes is not sufficient to allow navigation tasks without additional processing of the visual input. In this study, we simulated a low resolution array (15 × 18 electrodes, similar to a forthcoming generation of arrays) and evaluated the navigation abilities restored when visual information was processed with various computer vision algorithms to enhance the visual rendering. Three main visual rendering strategies were compared to a control rendering in a wayfinding task within an unknown environment. The control rendering corresponded to a

resizing of the original image onto the electrode array size, according to the average brightness of the pixels. In the first rendering strategy, vision distance was limited to 3, 6, or 9 m, respectively. In the second strategy, the rendering was not based on the brightness of the image pixels, but on the distance between the user and the elements in the field of view. In the last rendering strategy, only the edges of the environments were displayed, similar to a wireframe rendering. All the tested renderings, except the 3 m limitation of the viewing distance, improved navigation performance and decreased cognitive load. Interestingly, the distance-based and wireframe renderings also improved the cognitive mapping of the unknown environment. These results show that low resolution implants are usable for wayfinding if specific computer vision algorithms are used to select and display appropriate information regarding the environment. **Key Words:** Visual neuroprostheses—Retinal implant—Spatial cognition—Navigation—Wayfinding—Computer vision—Blind.

Visual neuroprostheses (1) elicit visual perception through microstimulation in various locations of the visual system, such as the primary visual cortex (2), the optic nerve (3), and the retina (4). Traditionally, the input from a camera is processed by a computer and converted into microstimulations that elicit phosphenes via an electrode array (5). The most advanced implants to date are the retinal implants like the Argus II (Second Sight Medical Products, Inc., Sylmar, CA, USA). This epiretinal implant stimulates the retina via 60 electrodes, providing a very low visual resolution. Mobility tasks

such as finding a black door on a white wall or following a white line on a dark floor showed that the implant slightly improved subjects' performance compared to chance (6). The resolution is increasing slowly in the range of a hundred phosphenes and important challenges remain to improve their functional benefits (7).

On the contrary, the domain of image processing is improving at a fast pace. Embedding high level image processing algorithms could lead to great enhancements in the visual perceptions restored by current low resolution implants (8). To explore the benefits from image processing in the usability of low resolution visual implants, a convenient solution is to use simulated prosthetic vision [SPV]. Rendering in a head-mounted display is guided by phosphene descriptions reported by implanted patients (9). SPV offers two main advantages: (i) usability of low resolution implants can be tested

doi: 10.1111/aor.12868

Received March 2016; revised August 2016; accepted August 2016.

Address correspondence and reprint requests to Marc J.-M. Macé, IRIT-ELIPSE, Université P. Sabatier, 118 Route de Narbonne, 31062 Toulouse Cedex 9, France. E-mail: Marc.Mace@irit.fr

without involving implanted patients (10) and (ii) it is possible to anticipate implant development in order to assess the minimal properties required to achieve a specific task (11). Various strategies have been explored to optimize SPV rendering. This was especially the case for reading capabilities (12), object grasping (13), or localization tasks (14).

In the first mobility study in 1992, Cha et al. (11) concluded that 625 phosphenes and a camera field of view of 30° were required to reach acceptable performances. More recent studies also focused on obstacle avoidance in a corridor (15,16). It has been shown that artificial vision algorithms that highlight obstacles (17) or planar surfaces (18) improve the preferred walking speed (19). Dagnelie et al. (20) designed a virtual environment with a high contrast between the ground and the walls. They evaluated the impact of background noise and electrode dysfunction, and observed a great variability between subjects and a slight effect of the electrode dropout rate. Rheede et al. (21) also used a virtual environment to check if subjects were able to follow instructions and walk through a predetermined path. The results illustrated the importance of peripheral information, and also that visual field distortion can lead subjects to misinterpret what they see.

All those studies focused on mobility and obstacle avoidance. To our knowledge the wayfinding task has never been addressed in SPV. Even in the studies by Dagnelie et al. (20) and Rheede et al. (21), the comprehension of the environment was not necessary for the subjects to follow a predetermined path. Successful wayfinding is based on the perception of specific cues from the environment (landmarks), but also on the selection of an appropriate path (22). All these tasks are difficult to perform with low resolution implants, which points out the need to highlight pertinent information within the surroundings. Indeed, in a recent experiment, Vergnieux et al. (23) showed that wayfinding with a simple image resizing poses great difficulties, and that performance is improved when the contrast between the ground and the walls is enhanced. To explain this result, we posit that perception through prosthetic vision, that is, with low resolution and low contrast, quickly gets overcrowded. This congestion hinders the comprehension of the environment, and, furthermore, prevents the identification of landmarks that are needed for wayfinding.

In the current experiment, we tested the hypothesis that limiting the cues that are rendered in prosthetic vision may improve the comprehension of the scene, and hence enhance wayfinding

performance. McCarthy et al. showed that it is possible to enhance structural information (24) or surface boundaries (25) with visual algorithms. We designed a wayfinding task within a virtual environment similar to an urban neighborhood. The subjects perceived the scene via different renderings that specifically enhance proximal or structural cues. The results show that both embedded algorithms improved the behavioral performance and minimized the mental workload, but also allowed the elaboration of a more reliable mental representation of the explored environment.

MATERIALS AND METHODS

Subjects

Fourteen subjects (five females and nine males aged from 18 to 31) with normal vision participated in the experiment. This experiment was conducted according to the ethical recommendations of the Declaration of Helsinki and was approved by a local ethical committee (CLERIT, University of Toulouse). All subjects gave written informed consent to participate.

Experimental setup

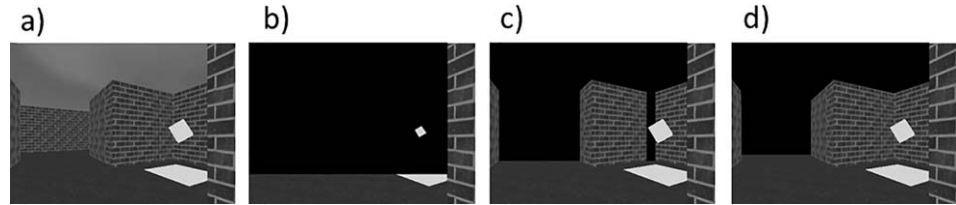
The virtual environment was displayed in a head mounted display (NVisor SX-60 HMD; NVis Inc., Reston, VA, USA) with a visual angle of $24 \times 17^\circ$ for all conditions.

The orientation of the virtual camera was locked to the subject's head orientation with a motion capture system (OptiTrack; NaturalPoint Inc., Corvallis, OR, USA). The subjects used the arrows of the keyboard to travel within the virtual environment. The up arrow was used to go forward. The left and right keys were used to turn.

When implementing a simulator of prosthetic vision, there is often a trade-off between realism and usability. Tracking the eye's position to stabilize the phosphenes on the retina better reflects the perception of an implanted patient. However, this generates a higher discomfort for the subject (motion sickness), and frequent recalibrations are needed (especially within a VR helmet), which interrupts the experiment. As we chose to limit subject discomfort and favor natural head motions to interact within the virtual environment, we ruled out the possibility to lock the display to the gaze. Similar choices were made in recent studies (see, e.g., [20,26]).

Each environment was restricted to a $45 \text{ m} \times 45 \text{ m}$ area, and contained three building blocks, and 33 turns on average (max = 36,

FIG. 1. Nonprosthetic renderings: (a) IRR-Control; (b–d) IRR-3, IRR-6, and IRR-9 renderings, respectively. The four illustrations are derived from the same point of view.



min = 28). All the turns were 90°. The paths within the environment were all 5 m wide. We built 12 different but comparable environments by shuffling these constitutive elements.

Experimental conditions

Ten renderings were used in this study: four were based on the regular rendering provided by the Irrlicht engine (IRR), and six were based on SPV.

IRR renderings

All the IRR renderings were generated with Irrlicht 3D open source game engine (27). We designed three conditions where the vision depth was limited to three different distances (3, 6, and 9 m) after which any visual information was hidden. The four IRR renderings were:

- Irrlicht control (IRR-Control). The regular IRR rendering, used without any alteration and no depth limitation.
- Limited Irrlicht (IRR-3, IRR-6, and IRR-9). We used the Irrlicht built-in fog feature to conceal any visual information beyond 3, 6, or 9 m from the position of the virtual camera. Anything that was further away was hidden by a black surface (see Fig. 1).

SPV renderings

The phosphenes were round dots with a Gaussian profile and a radius of one degree of visual angle. The array consisted of 18×15 phosphenes and we used four levels of luminance. A dropout rate of 10% was added to simulate electrodes malfunction. Retinal adaptation was simulated by switching rapidly (100 ms) off and on the phosphenes that displayed a constant gray level for more than 1 s. In all the SPV renderings, the objects related to the task (jewels and base) were displayed with the brightest luminance level.

In addition to the control rendering, we designed five other SPV conditions (Fig. 2). Three of them (3, 6, and 9 m) correspond to the three Irrlicht-based conditions with proximal vision only. The two last renderings were based on specific

algorithms and were called SPV-Distance and SPV-Wireframe.

- SPV-NoLimit: a plain re-sample of the regular Irrlicht view that matches the resolution and properties of the phosphene array. The brightness of a phosphene matches to the average brightness of the corresponding image pixels.
- SPV-3, SPV-6, and SPV-9: renderings based on a re-sampling of the image but the elements further away than 3, 6, or 9 m, respectively are hidden. Here again, the brightness of the phosphenes matches to the average brightness of the corresponding image pixels.
- SPV-Distance: in that rendering, phosphene luminance corresponds to the distance of scene elements, not to their brightness. Elements closer than 3 m are rendered with light gray. Elements between 3 and 9 m appear as dark gray. Everything beyond 9 m is black.
- SPV-Wireframe: in this rendering, the edges of the different surfaces of the environment are highlighted. The ground and the walls are black and the edges between the ground and the walls or between two walls are light gray.

Task and observed variables

Subjects had to collect and bring back to the starting base six jewels in less than 5 min. They could carry only two jewels simultaneously. Hence they had to return to the starting base at least three times to complete the task. Two aims were explicitly mentioned: 1) completing the task as fast as possible; 2) memorizing the whole layout of the environment, including the position of the six jewels. Subjects came twice to the lab, each session lasted 2 h. The conditions were distributed within the two sessions with five conditions per session. In order to acknowledge that subjects clearly understood how the environments were built, they all began with the IRR-Control condition (unmodified scene view). According to our hypothesis, the most difficult condition should be SPV-NoLimit; hence this condition systematically occurred in the middle of a session. Apart from these light rules, the

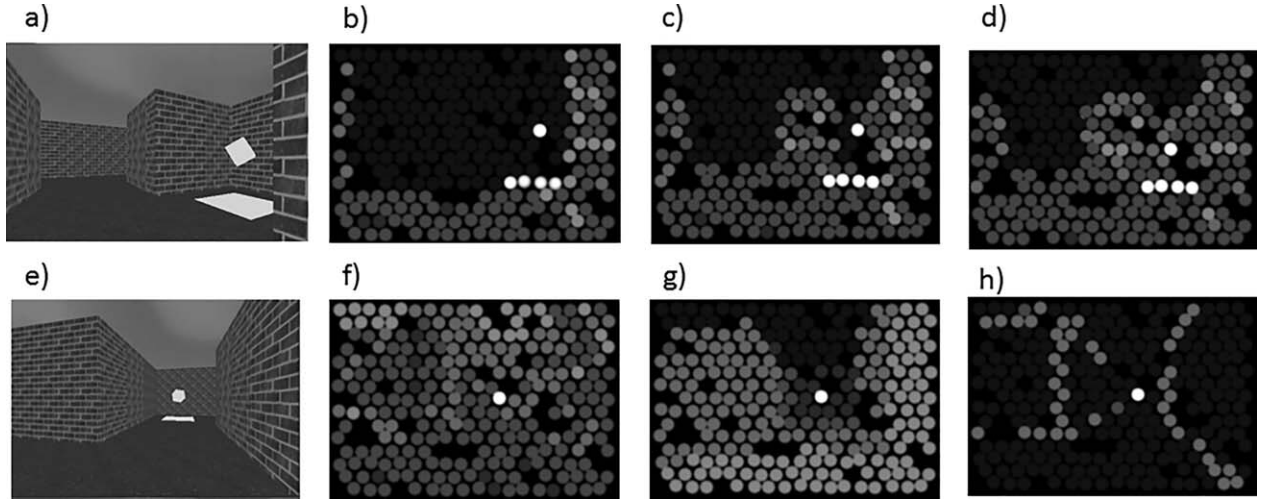


FIG. 2. Simulated prosthetic vision renderings. (a) IRR point of view with corresponding SPV-3 (b), SPV-6 (c), and SPV-9 (d) renderings. (e) Another IRR point of view with corresponding SPV-NoLimit (f), SPV-Distance (g), and SPV-Wireframe (h) renderings.

conditions were randomly distributed within the two sessions.

We used a performance index (PI) that measures each subject's performance relative to the best performance across all subjects and conditions. This index goes from 0 (no jewels collected) to 100 (shortest time to collect all six jewels) and is computed as follows:

$$PI = \frac{J_i - J_{\text{MIN}}}{J_{\text{MAX}} - J_{\text{MIN}}} \times 50 + \frac{T_{\text{MAX}} - T_i}{T_{\text{MAX}} - T_{\text{MIN}}} \times 50.$$

J_i is the number of collected jewels during the current trial, J_{MIN} is the minimal number of collected jewels (here $J_{\text{MIN}}=0$), J_{MAX} is the maximal number of collected jewels (here $J_{\text{MAX}}=6$), T_i is the completion time for the current trial, T_{MIN} is the shortest trial completion time among all subjects and conditions, and T_{MAX} is the longest trial completion time (here $T_{\text{MAX}}=5$ min).

Completion time and number of collected jewels were recorded to compute the PI for each trial. If a subject brings back the six jewels in exactly 5 min, then the PI is equal to 50. If a subject collects less than six jewels in 5 min, the PI is lower than 50.

In addition to the PI, we assessed the mental spatial maps acquired during the exploration of the environment. Subjects explored a different environment for each condition, which means that each of them had explored 10 different environments when they had completed the whole experiment. For each condition, subjects performed the navigation task twice and they were asked to draw a map of the environment after those two trials. Four external judges who were unaware of the experimental

conditions and hypotheses made an evaluation of the drawings. We asked them to score the drawings from 0 to 10 based on similarity with the real 2D maps of the environments. They were explicitly asked to base their evaluation on the topological properties of the drawings rather than their metric properties. In addition we recorded the number of collisions with the walls. We also measured the cognitive load associated to each rendering using the Nasa-TLX questionnaire (28) after each condition.

Hypotheses

According to previous results (29), decreasing the viewing distance in Irrlicht conditions should impair wayfinding performance and cognitive mapping. According to our main hypothesis, which was based on (23), we made the general assumption that limiting vision depth in the SPV renderings would not decrease the wayfinding performance, but, on the contrary, would improve it, because the visual percept is less crowded, and hence more understandable. Then decreasing the viewing distance (SPV-9 to SPV-6 and SPV-3) should reduce the visual congestion, and hence improve the wayfinding performance. In addition, a better comprehension of the scene should reduce the cognitive load during the task and lead to a better cognitive mapping of the whole environment.

With the SPV-Distance and SPV-Wireframe renderings, we aimed at showing that minimizing the rendering to specific cues that are useful for a wayfinding task (i.e., cues of distance or structure) would improve the performances. The SPV-Distance rendering should help to perceive different planes within the environment. The wireframe

representation is a valuable abstraction of the 3D environment (30), and should help to understand the local configuration of corridors and crossings. Hence, we made the hypothesis that these renderings would improve the wayfinding performance (PI), but also the quality of the mental representation of the environment (drawing score).

All statistical tests were computed with the software R from the R Foundation (31). As the distributions were not normal, we used Wilcoxon tests (32) with Bonferroni corrections for multiple comparisons.

RESULTS

Performance

As expected, subjects' performance increases when the viewing distance is extended from 3 m to "infinity." Significant differences were found between the average PI for the condition IRR-3 ($M = 59.5$, $SD = 14.0$) and the other ones: IRR-6 ($M = 74.7$, $SD = 8.6$, $P < 0.01$), IRR-9 ($M = 76.2$, $SD = 7.8$, $P < 0.001$), and IRR-Control ($M = 80.5$, $SD = 4.5$, $P < 0.001$). There was no statistical difference between IRR-6, IRR-9, and IRR-Control conditions.

Most of the subjects could not bring back all the jewels in time for SPV-NoLimit ($M = 37.3$, $SD = 17.2$) and SPV-3 ($M = 38.4$, $SD = 18.4$) conditions. The average PI is above 50% for SPV-6 ($M = 63.6$, $SD = 24.0$), SPV-9 ($M = 50.5$, $SD = 22.0$), SPV-Distance ($M = 57.2$; $SD = 22.3$), and SPV-Wireframe ($M = 65.8$, $SD = 19.4$) conditions, which indicates that the subjects were able to bring back the six jewels within 5 min.

Significant differences appeared between condition SPV-3 and conditions SPV-6 ($P < 0.001$), SPV-Distance ($P < 0.001$), and SPV-Wireframe ($P < 0.001$), respectively. The differences between SPV-6 and SPV-NoLimit ($P < 0.01$), and between SPV-9 and SPV-Wireframe ($P < 0.05$) were significantly different too. Finally, the condition SPV-NoLimit differed significantly from conditions SPV-Distance ($P < 0.01$) and SPV-Wireframe ($P < 0.001$). All those results are shown in Fig. 3.

We observed a very high number of collisions with the walls in the SPV-NoLimit condition ($M = 47.1$, $SD = 27.8$), which is significantly different from SPV-3 ($M = 14.0$, $SD = 20.6$, $P < 0.01$), SPV-6 ($M = 8.1$, $SD = 5.5$, $P < 0.001$), SPV-Distance ($M = 3.5$, $SD = 3.5$, $P < 0.001$), and SPV-Wireframe ($M = 9.5$, $SD = 8.9$, $P < 0.01$) conditions. SPV-Distance ($M = 3.5$, $SD = 3.5$) and SPV-9 ($M = 16.5$, $SD = 9.7$, $P < 0.001$) are also significantly different.

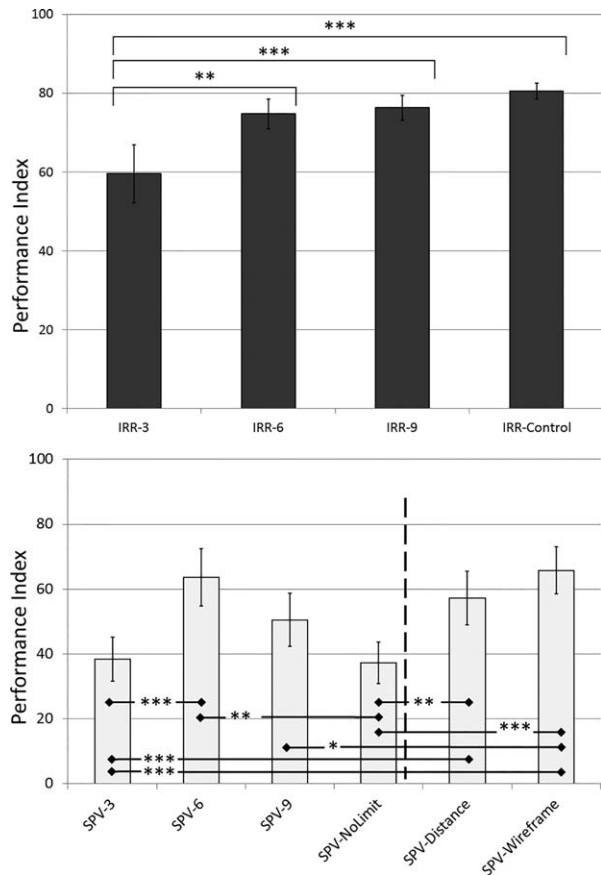


FIG. 3. Mean performance indexes. Error-bars are 95% confidence intervals. The upper panel gives the Performance Indexes for the different nonprosthetic vision conditions. The bottom panel plots the Performance Indexes for the different simulated prosthetic vision conditions. The dashed line separates limited vision SPV conditions from the ones with enhanced cues (* $P < 0.05$; ** $P < 0.01$; *** $P < 0.001$).

Cognitive load

As a reminder, a cognitive load of 100 means an extremely difficult task and a cognitive load of 0 means an effortless task. Among the Irrlicht renderings, the rendering raising the highest cognitive load was the IRR-3 ($M = 46.1$, $SD = 15.0$). This condition significantly differs from IRR-6 ($M = 27.0$, $SD = 11.0$, $P < 0.001$), IRR-9 ($M = 25.4$, $SD = 12.1$, $P < 0.001$), and IRR-Control ($M = 23.7$, $SD = 11.9$, $P < 0.001$). There were no other statistical differences among the Irrlicht conditions. The SPV condition with the highest cognitive load was the SPV-NoLimit condition ($M = 74.3$, $SD = 23.7$), followed by the SPV-3 condition ($M = 61.6$, $SD = 14.5$). SPV-6 ($M = 49.2$, $SD = 13.7$), SPV-9 ($M = 53.4$, $SD = 12.5$), and SPV-Distance ($M = 50.0$, $SD = 16.5$) yielded a similar cognitive load around 50. The lowest cognitive load was observed for the SPV-Wireframe condition ($M = 38.6$, $SD = 16.2$). We

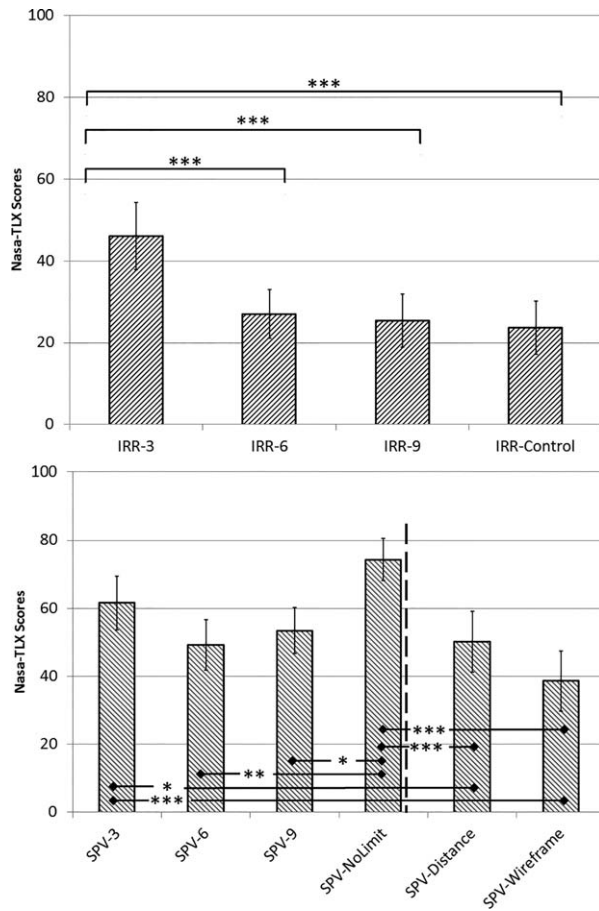


FIG. 4. Nasa-TLX scores. An important score implies an important cognitive workload. So, the easiest conditions received the lowest scores. Error bars are 95% confidence intervals. The upper panel shows the scores for the nonprosthetic conditions. The bottom panel plots the scores for the simulated prosthetic vision conditions. The dashed line separates simulated prosthetic vision conditions with limited vision from the ones with enhanced cues (* $P < 0.05$; ** $P < 0.01$; *** $P < 0.001$).

observed statistical differences between SPV-NoLimit and SPV-6 ($P < 0.01$), SPV-9 ($P < 0.05$), SPV-Distance ($P < 0.001$), and SPV-Wireframe ($P < 0.001$). In addition, scores for SPV-3 are different from the ones observed with SPV-Distance ($P < 0.05$) and SPV-Wireframe ($P < 0.001$). We plotted those results in Fig. 4.

Map drawing scores

When looking at Irrlicht conditions only, the subjects produced the poorest drawings after exploration with the IRR-3 rendering ($M = 4.3$, $SD = 2.6$). The drawing scores then progressively improve with increasing viewing distance. Mean scores for the IRR-6 ($M = 6.8$, $SD = 2.7$) and IRR-9 ($M = 7.6$, $SD = 2.7$) conditions were lower than the scores for

the IRR-Control condition ($M = 8.4$, $SD = 1.6$). Statistical differences appear between IRR-3 and IRR-9 ($P < 0.001$) as well as between IRR-3 and IRR-Control ($P < 0.001$).

The whole pattern was different for the SPV-renderings. Subjects reported the highest scores with the condition SPV-Wireframe ($M = 4.6$; $SD = 3.3$), which differs significantly from conditions SPV-3 ($M = 2.2$; $SD = 2.7$; $P < 0.05$) and SPV-NoLimit ($M = 1.3$; $SD = 1.6$; $P < 0.01$). SPV-Distance ($M = 3.8$; $SD = 3.6$) was the second best condition, and significantly differs from SPV-NoLimit ($P < 0.05$). Lowest scores were obtained with the condition SPV-NoLimit ($M = 1.3$; $SD = 1.6$). Conditions SPV-6 ($M = 2.5$; $SD = 1.9$) and SPV-9 ($M = 2.8$; $SD = 2.7$) were in between, and do not differ significantly from the other conditions. The drawing scores are plotted in Fig. 5.

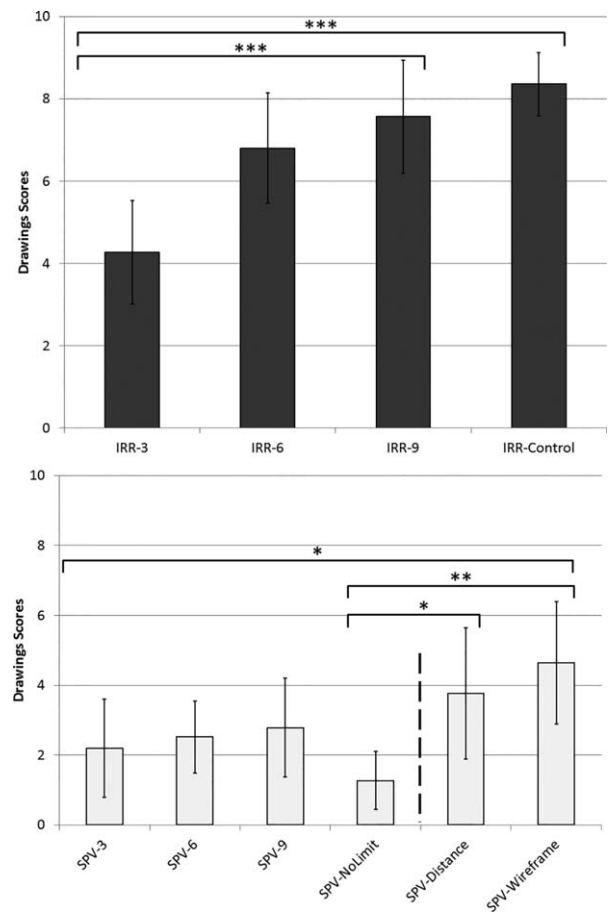


FIG. 5. Drawing scores. Error bars are 95% confidence intervals. The upper panel shows the drawings scores for the nonprosthetic vision. The bottom panel plots the drawing scores for simulated prosthetic vision conditions. The dashed line separates simulated prosthetic vision conditions with limited vision from the ones with enhanced cues (* $P < 0.05$; ** $P < 0.01$; *** $P < 0.001$).

DISCUSSION

Design of the prosthetic renderings

All the renderings provided the same visual span ($24 \times 17^\circ$), close to the visual span of retinal implants (33). The phosphenes were round dots with a Gaussian profile and a radius of one degree of visual angle. The array consisted of 18×15 phosphenes, a resolution that is in line with the announcement of the next generation of Second Sight's epiretinal implant (8). We used only four levels of luminance for each phosphene. Indeed, even though some implanted subjects are able to discriminate 10 luminance levels (34), this performance is reached by a minority of patients (35). We also added a 10% dropout rate to simulate electrode malfunction (6). Finally, we simulated retinal adaptation by switching rapidly (100 ms) off and on the phosphenes that displayed a constant luminance (gray level) for more than 1 s (36). SPV-Wireframe rendering was inspired by recent artificial vision results showing that it is possible to determine the relative position of the floor and buildings in urban scenes in real time (25,37).

Visual perception and behavioral decisions within the environment

With nonprosthetic renderings (Irrlicht conditions), subjects managed to complete the task and showed good ($60\% < \text{PI} < 80\%$) to very good ($\text{PI} > 80\%$) performances. Although the PI slightly decreased, it was not different when comparing IRR-Control (80.5), IRR-9 (76.2), and IRR-6 (74.7) conditions. Subjects had significantly more difficulties with the IRR-3 rendering condition but still managed to bring back all the jewels in time ($\text{PI} = 59.5$). The cognitive load that they reported was very coherent with the behavior. It was very low (Nasa-TLX < 27) for IRR-Control, IRR-9, and IRR-6, and had a tendency to increase when the seeing distance was reduced. The cognitive load for the IRR-3 condition was significantly higher than for the other Irrlicht conditions. Taken together, these results confirm that subjects are able to find their way in an unknown virtual environment, even in absence of kinesthetic cues related to walking (38). However when the seeing distance is too short (restricted to 3 m in our experiment), the wayfinding performance is low, and the corresponding cognitive load is very high.

Results obtained with the simulated prosthetic renderings present a completely different pattern. The SPV-NoLimit condition (i.e., with the greater seeing distance) appeared as the most difficult

condition overall, with the lowest PI ($M = 37.3$) as well as the highest Nasa-TLX score ($M = 74.3$) and the highest number of collisions ($M = 47.1$). This means that subjects had major difficulties to understand the environment and find their way with this rendering. It is probably a consequence of the overcrowded prosthetic percept that is provided by a limited number of phosphenes (270 phosphenes) with a limited number of luminance levels (only four levels). Low resolution and low contrast result in a difficulty to perceive any difference between the ground, the walls, and the sky. Moreover, subjects lack the visual feedback needed to integrate their own movements. As a consequence they have difficulties understanding what they see and where they go.

When the viewing distance decreases, the wayfinding performance improves. Indeed, between SPV-NoLimit, SPV-9, and SPV-6, the PI increases from 37.3 to 50.5, and 63.6, respectively. The corresponding Nasa-TLX scores followed a symmetric trend. These results confirm our main hypothesis stating that reducing the viewing distance in the simulated prosthetic rendering improves perception and wayfinding. The limitation of viewing distance has two consequences on the visual rendering: it conceals the distant visual cues, which simplifies the visual rendering, but it also creates a contrast feature within the rendering corresponding to the borders with the remaining visual elements. The subjects probably used both cues to understand the visual scene, which raises the question of their relative importance. This question may be addressed in a future study. Nevertheless, it is important to note that this contrast appears without detecting the border per se, and that it would also appear for an implanted patient using prosthetic vision with the same algorithms.

It appears that there is an optimal viewing distance around 6 m in our environments for the simulated prosthetic rendering. The main explanation lies in the low resolution of the SPV in general. The subjects often simply fail to understand the percepts. For instance, they are not able to identify the intersections, which results in less efficient wayfinding behavior and less accurate mental maps. Of course the perceptual difficulties lead to increased cognitive load during the wayfinding task. When the viewing distance is decreased, the percept provided by the SPV gets less and less crowded. In the optimal condition (SPV-6 rendering in our experiment), the subjects could more easily detect intersections and use them as local landmarks during navigation. In comparison, the

performance observed with the SPV-3 rendering was very low (i.e., comparable to the performance observed with the SPV-NoLimit rendering). In fact, distant visual information was also simplified in the SPV-3 condition, which should improve the navigation performance. However, the remaining proximate visual information was too restricted to understand the intersections in the maze, which probably counteracts the simplification effect, and explains the low performance in this condition.

With the distance-augmented rendering, the phosphene luminance corresponds to the distance of scene elements, not to their brightness. With that rendering, subjects performed better than with most of the limited distance SPV renderings. The PI observed in that condition ($PI = 57.2$) was very close to the performance observed with SPV-6 ($PI = 63.2$). Subjects could easily detect intersections as far as 9 m and move quickly in the environment. The performance and the cognitive load (Nasa-TLX = 50.1) associated to the wayfinding task were similar to those observed with the SPV-6 rendering.

The best PI observed with SPV was obtained with the SPV-Wireframe rendering ($PI = 65.8$). As opposed to the other SPV conditions, the SPV-Wireframe rendering is not dependent on distance. The rendering provides a quite clear outline of the edges of the walls around them, which is a good representation of the reality (30). The perspectives are also perceivable, and help to understand the configuration of the surroundings (39). Although this rendering relies only on three levels of luminance, subjects were able to detect and identify distant intersections. It is thus quite easy to understand the visual scene, keep walking in a specific direction, and find one's way.

Cognitive mapping with enhanced prosthetic vision

In our experiment, we observed how different rendering conditions of SPV improved the construction of mental maps during the exploration of a maze. The drawing scores observed after the Irrlicht conditions improved with greater seeing distances, from IRR-3 ($M = 4.3$) to IRR-Control ($M = 8.4$). In those conditions the farther the subjects could see, the easier they could build a mental representation of the explored environment. When subjects' view is restricted to a limited distance, they can only see a limited portion of the scene. Then, subjects had to better integrate their own movement, which increases the difficulty of the task. The increasing cognitive load from IRR-

Control to IRR-9, IRR-6, and IRR-3 conditions could reflect this integration process.

The results were different for the SPV conditions because more accurate drawings were obtained for the SPV-Distance and SPV-Wireframe renderings, and lower cognitive load scores were obtained for SPV-Distance, SPV-Wireframe, and SPV-6. For the SPV-NoLimit condition, the map drawing score was very low ($M = 1.3$). In that condition, the only elements that were easy to identify were the jewels and the base that were brighter; but they disappeared after being picked up. As it was very difficult to recognize any landmark, the subjects were not able to build a correct mental representation of the maze. For the limited viewing distance conditions, subjects still had difficulties to build a cognitive map (drawing scores of 2.2, 2.6, and 2.8 for SPV-3, 6, and 9, respectively). Although the SPV-6 rendering improves the behavioral performance within the maze, it does not allow a significantly better map drawing score than the initial SPV-NoLimit rendering. This means that this rendering is sufficient to navigate an unknown environment, but not to identify and memorize landmarks, and hence build an effective mental representation of the maze. One explanation is that the visual elements of the maze, such as intersections, are easily detectable with this rendering. This rendering is sufficient to perform mobility but is still not optimal to build a mental representation of the maze.

The map drawing score obtained for the SPV-Distance condition ($M = 3.8$) is significantly higher than the score for the SPV-NoLimit condition. With this rendering, the intersections can be detected as far as 9 m, and subjects can easily move. The map drawing scores obtained for the SPV-Wireframe condition ($M = 4.6$) are the highest scores observed with the SPV renderings, and are significantly different from those observed for SPV-3 and SPV-NoLimit renderings. As already mentioned, the local structure of the maze was easily perceivable with this rendering. First, there was no depth limitation. Second, the subjects were able to identify specific landmarks (such as the configuration of a specific crossing). The visual percepts provided by this rendering are sparse but they are meaningful. In addition, the perspective provided by the edges allowed the subjects to infer distances. With an unlimited seeing distance and the absence of crowding within the visual percept, subjects had fewer difficulties to construct mental maps of the environment.

This experiment was performed in a virtual environment. The next step would be to validate the

results in a real environment with a mobile simulator of prosthetic vision. In addition, because the renderings are now more specific to the ongoing task (e.g., navigation with the wireframe rendering), it would also be interesting to check that the subjects are able to switch between different renderings (e.g., switching between navigation and object grasping, see [40], or face recognition, see [14]). Finally, it would be essential to evaluate the ability of implanted patients to use those renderings in real situations.

CONCLUSION

In simulated prosthetic vision, only a few studies focused on navigation tasks (20,23). With a low resolution implant, rendering the visual scene with no specific processing leads to visual overcrowding, and does not provide visual cues sufficient to navigate an unknown environment. We designed and evaluated different renderings that simplify the visual information rendered by the implant. The first strategy consisted of limiting the seeing distance. With this rendering, subjects showed better behavioral performance, and the cognitive load during navigation was decreased. The second strategy consisted of rendering the distance to the elements instead of their brightness. The results were slightly better than the results observed with the limited seeing distance rendering. A more beneficial strategy consisted of rendering only the edges that are present in the environment. This rendering increased the navigation performance, decreased the cognitive load, but also improved the cognitive mapping of the unknown environment. This rendering has not been evaluated in real conditions, which should be done before reporting definitive conclusions. Nevertheless, this study suggests that embedding appropriate specific renderings in visual prosthesis might restore valuable sensory and cognitive abilities. Specifically, our experiment showed that, even with low resolution implants that have less than 300 electrodes, implanted patients should be able to navigate unknown environments if the edges of the environment are detected, and enhanced in the rendering. It is probable that a set of several algorithms is needed to assist the implanted patients in completing all the different daily tasks.

Author Contributions: Victor Vergnien contributed to the concept and design of the experiment,

data collection, statistics, data analysis and interpretation, and drafting the article. Marc J.-M. Macé and Christophe Jouffrais contributed to the concept and design of the experiment, critical revision of this article, data analysis and interpretation, and approval of the article.

Conflict of Interest: The author reports no conflict of interest.

REFERENCES

1. Dobelle WH, Mladejovsky MG, Girvin JP. Artificial vision for the blind: electrical stimulation of visual cortex offers hope for a functional prosthesis. *Science* 1974;183:440–4.
2. Brindley GS, Lewin WS. The sensations produced by electrical stimulation of the visual cortex. *J Physiol* 1968;196: 479–93.
3. Veraart C, Raftopoulos C, Mortimer JT, et al. Visual sensations produced by optic nerve stimulation using an implanted self-sizing spiral cuff electrode. *Brain Res* 1998; 813:181–6.
4. Zrenner E. Fighting blindness with microelectronics. *Sci Trans Med* 2013;5:210ps16.
5. Zhou DD, Dorn JD, Greenberg RJ, The Argus® II retinal prosthesis system: an overview. *Multimedia and Expo Workshops (ICMEW), 2013 IEEE International Conference*, 2013;1–6.
6. Humayun MS, Dorn JD, da Cruz L, et al. Interim results from the international trial of Second Sight's visual prosthesis. *Ophthalmology* 2012;119:779–88.
7. Picaud S, Sahel J-A. Retinal prostheses: clinical results and future challenges. *C R Biol* 2014;337:214–22.
8. Stronks HC, Dagnelie G. The functional performance of the Argus II retinal prosthesis. *Expert Rev Med Dev* 2014; 11:23–30.
9. Dagnelie G, Stronks HC. Prosthetic vision, perceptual effects. In: Jaeger D, Jung R, eds. *Encyclopedia of Computational Neuroscience*. New York: Springer, 2014;1–4.
10. Dagnelie G, Thompson RW, Barnett DG, Zhang W. Simulated prosthetic vision: perceptual and performance measures. *Vis Sci Its Appl* 2001:43–6.
11. Cha K, Horch KW, Normann RA. Mobility performance with a pixelized vision system. *Vis Res* 1992;32:1367–72.
12. Pérez Fornos A, Sommerhalder J, Pelizzone M. Reading with a simulated 60-channel implant. *Front Neurosci* 2011; 5:8.
13. Denis G, Macé MJ-M, Jouffrais C. Simulated prosthetic vision: object recognition and localization approach. *Proceedings of the 4th International Conference on Neuroprosthetic Devices (ICNPD 2012)*, 2012;40–1.
14. Wang J, Wu X, Lu Y, Wu H, Kan H, Chai X. Face recognition in simulated prosthetic vision: face detection-based image processing strategies. *J Neural Eng* 2014;11:11.
15. Barnes N, Lieby P, Dennet H, et al. Investigating the role of single-viewpoint depth data in visually-guided mobility. *J Vis* 2011;11:926.
16. Parikh N, Itti L, Humayun MS, Weiland J. Performance of visually guided tasks using simulated prosthetic vision and saliency-based cues. *J Neural Eng* 2013;10:13.
17. McCarthy C, Walker JG, Lieby P, Scott A, Barnes N. Mobility and low contrast trip hazard avoidance using augmented depth. *J Neural Eng* 2014;12:15.
18. McCarthy C, Barnes N. Surface extraction from iso-disparity contours. *Asian Conference on Computer Vision*, 2011;410–21.
19. Clark-Carter DD, Heyes AD, Howarth CI. The efficiency and walking speed of visually impaired people. *Ergonomics* 1986;29:779–89.

20. Dagnelie G, Keane P, Narla V, Yang L, Weiland JD, Humayun MS. Real and virtual mobility performance in simulated prosthetic vision. *J Neural Eng* 2007;4:S92–101.
21. Rheede JJV, Kennard C, Hicks SL. Simulating prosthetic vision: optimizing the information content of a limited visual display. *J Vis* 2010;10:32.
22. Meilinger T. The network of reference frames theory: a synthesis of graphs and cognitive maps. In: Freksa C, Newcombe NS, Gärdenfors P, Wöflf S, eds. *Spatial Cognition VI: Learning, Reasoning, and Talking about Space*. Berlin, Heidelberg: Springer-Verlag, 2008;344–60.
23. Vergnieux V, Macé MJ-M, Jouffrais C. Wayfinding with simulated prosthetic vision: performance comparison with regular and structured-enhanced renderings. *36th Annual International Conf. of the IEEE EMBS*, 2014;2585–8.
24. McCarthy C, Feng D, Barnes N. Augmenting intensity to enhance scene structure in prosthetic vision. *2013 IEEE International Conference on Multimedia and Expo Workshops (ICMEW)*. IEEE, 2013;1–6.
25. McCarthy C, Barnes N, Lieby P. Ground surface segmentation for navigation with a low resolution visual prosthesis. *Annual International Conference of the IEEE Engineering in Medicine and Biology Society*, 2011;4457–60.
26. Zapf MPH, Boon M-Y, Matteucci PB, Lovell NH, Suaning GJ. Towards an assistive peripheral visual prosthesis for long-term treatment of retinitis pigmentosa: evaluating mobility performance in immersive simulations. *J Neural Eng* 2015;12:14.
27. Gebhardt N. Irrlicht Engine—A Free Open Source 3D Engine. <http://www.irrlicht.sourceforge.net>, 2010. Accessed July 1, 2016
28. Hart SG, Staveland LE. Development of NASA-TLX (Task Load Index): results of empirical and theoretical research. *Adv Psychol* 1988;52:139–83.
29. Barton K, Ellard C. Finding your way: the influence of global spatial intelligibility and field-of-view on a wayfinding task. *J Vis* 2009;9:1125.
30. Wolf MJ. Abstraction in the video game. In: Wolf MJ, Perron B, eds. *The Video Game Theory Reader*, Abingdon, UK: Routledge, 2003;47–66.
31. R Development Core Team. *R: A Language and Environment for Statistical Computing*. Vienna, Austria: R Foundation for Statistical Computing, 2010.
32. Hollander M, Wolfe DA. *Nonparametric Statistical Methods*, 2nd Edition. Hoboken, NJ: John Wiley & Sons, 1999.
33. Chen SC, Suaning GJ, Morley JW, Lovell NH. Simulating prosthetic vision: I. Visual models of phosphenes. *Vis Res* 2009;49:1493–506.
34. Humayun MS, Weiland JD, Fujii GY, et al. Visual perception in a blind subject with a chronic microelectronic retinal prosthesis. *Vis Res* 2003;43:2573–81.
35. Zrenner E, Wilke R, Zabel T. Psychometric analysis of visual sensations mediated by subretinal microelectrode arrays implanted into blind retinitis pigmentosa patients. *Invest Ophthalmol Vis Sci* 2007;48:659.
36. Wilke RG, Geppmaier U, Stingle K, Zrenner E. Fading of perception in retinal implants is a function of time and space between sites of stimulation. *Invest Ophthalmol Vis Sci* 2011;52:458.
37. Bauda M, Chambon S, Spangenberg M, Charvillat V. Segmentation de scènes urbaines par combinaison d'information. *ORASIS, Journée francophones des jeunes chercheurs en vision par ordinateur*, Cluny, 2013:8.
38. Riecke BE, Bodenheimer B, McNamara TP, Williams B, Peng P, Feureissen D. Do we need to walk for effective virtual reality navigation? Physical rotations alone may suffice. *Spatial Cognition VII*, 2010;234–47.
39. Gibson JJ. *The Ecological Approach to Visual Perception: Classic Edition*, New York: Psychology Press, 2014.
40. Macé MJ-M, Guivarch V, Denis G, Jouffrais C. Simulated prosthetic vision: the benefits of computer-based object recognition and localization. *Artif Organs* 2015;39: E102–E113.